Analysis of Sandwich Plates Using a Hybrid-Stress Finite Element

Koganti M. Rao* and H.-R. Meyer-Piening†
Institute for Lightweight Structures and Rope Ways, Zurich, Switzerland

The bending analysis of a generally orthotropic sandwich plate is presented using an accurate hybrid-stress finite element. The computer program necessary for such an analysis is developed, and its accuracy is checked by comparing the results with the three-dimensional elasticity solution of a simply supported three-layered rectangular laminate. The response of a square angle-ply, fiber-reinforced plastic-(FRP)-faced sandwich with simply supported and clamped edges is evaluated. The results show the following: 1) The soft core of an angle-ply FRP-faced thick sandwich supports a comparatively small amount of the shear force, more so with clamped conditions. The faces carry the shear force and are predominantly subjected to bending action about their centroidal axes, and hence, they no longer act as membranes. 2) To achieve the expected economy of the sandwich construction, it is recommended that the width-to-thickness ratio be kept greater than 20 and 50, respectively, in the cases of simply supported and clamped sandwich plates, wherever possible.

Nomenclature

a	= width of the sandwich plate
A_{ni}	= boundary of ith layer in element n
b	= length of the sandwich plate
B^i	= strain matrix of ith layer
C_d^i, C_S^i	= Boolean matrices corresponding to displacements and stresses, respectively, in ith layer
E_L, E_T, E_{xx} E_{zz}, E_{yy}	= elastic modulii, Eqs. (24) and (26)
G^i, G	= layer [Eq. (11b)] and element [Eq. (18b)] matrices
G_{LT}, G_{TT}, G_{xy} G_{yz}, G_{xz}	= shear modulii, Eqs. (24) and (26)
H^i, H	= layer [Eq. (11a)] and element [Eq. (18a)] matrices
h	= thickness of sandwich
$h_i (i = 1,2,3,4)$	= heights of layer boundaries measured from xy plane
$\|J\|$	= determinant of the Jacobian of coordinate transformation
k	= stiffness matrix, Eq. (22)
L	= longitudinal direction of fiber
N	= number of elements
N^i	= layer matrix depending on N_j and normalized coordinate ζ
N_j	= shape function of jth node
p	= transverse force intensity
p^i	= boundary load vector
p_0	= amplitude of sinusoidal load or uniformly distributed load
P_i	= 6×40 polynomial matrix, Eq. (2)
q^i, q	= layer and element nodal displacement vectors, respectively
Q^i, Q	= layer and element nodal force vectors, respectively
S	= width-to-thickness ratio, $= a/h$
S_i	= compliance matrix of ith layer
t_i	= half the thickness of ith layer
T	= transverse direction of fiber
$\bar{u}, \bar{v}, \bar{w}$	= normalized displacement components, Eq. (25)
u^i, v^i, w	= displacement components of ith layer
u_j^i, v_j^i, w_j	= values of u^i, v^i, w at jth node
U^i	= displacement vector of ith layer
V_{ni}	= volume of ith layer in element n
x, y, z	= global coordinate axes
x_j, y_j	= in-plane global coordinates of jth node
$\bar{z}$	= normalized value of z, $= 2z/h$
β, β^i	= element and layer stress parameter vectors, respectively
$\beta_j^i (i = 1,2,3)$	= components of β, Eq. (16)
ϵ_i	= strain vector of ith layer
$\epsilon_x, \epsilon_y, \epsilon_z, \epsilon_{yz}$, $\epsilon_{zx}, \epsilon_{xy}$	= engineering strains
θ	= fiber orientation angle measured from x axis
$\mu_{LT}, \mu_{TT}, \mu_{xy}$, μ_{yz}, μ_{zx}	= Poisson's ratios, Eqs. (24) and (25)
ξ, η, ζ	= normalized coordinates
Π	= hybrid-stress functional
σ_i	= stress vector of ith layer
$\sigma_x, \sigma_y, \sigma_z, \tau_{yz}$, τ_{zx}, τ_{xy}	= stress components
$\bar{\sigma}_x, \bar{\sigma}_y, \bar{\sigma}_z, \bar{\tau}_{yz}$, $\bar{\tau}_{zx}, \bar{\tau}_{xy}$	= normalized stress components

I. Introduction

THE development of plastic foam core material and fiber-reinforced plastic (FRP) composite technology led to the application of sandwich structures to new areas like ship building, automobile, chemical vessels, consumer goods, etc. The structural geometry in these areas is quite different from that of sandwiches used in space crafts as a result of varied design criteria: The face sheets and, as a whole, the sandwich walls are usually thicker. The detailed analysis of such structures needs refined modeling of their mechanical behavior. An attempt in that direction is made here.

Since the work of Reissner,[1] many research papers have been published on the topic. Improving on the theory of Hoff,[3] Yu[2] developed a new theory of elastic sandwich plates with arbitrary relative thicknesses and material properties of the face sheets and core. Rao[7] derived improved equations

Received Sept. 26, 1989; revision received July 12 1990; accepted Aug. 1, 1990.

*Assistant Professor, Mechanical Engineering Department, Indian Institute of Technology, Kharagpur, India.
†Professor.

governing the deflection of unsymmetric sandwich beams with a stiff core. Rao[8] and Rao and Meyer-Piening[9] evaluated the buckling analysis of FRP-faced sandwich panels. Mindlin[10] examined the domain of applicability of Reissner's sandwich plate equations by means of the reduction of higher-order approximation. A parametric differentiation technique was used by Rao and Valsarajan[11] to analyze the skew sandwich plates. Whitney[6] presented a procedure for calculating accurately the mechanical response of sandwich plates by modifying the classical laminated plate theory to include the effect of transverse shear deformation. The most accurate analysis of sandwich plates using the three-dimensional theory of elasticity approach was presented by Srinivas and Rao[4] and Pagano.[5]

The scope of application of the analytical solutions mentioned and others not cited is mainly limited to the cases of simple loading, geometry, and boundary conditions. To overcome this limitation, the more general finite element solution method has been adopted by many investigators for the analysis of sandwich structures. A four-noded rectangular element with 16 degrees of freedom based on a displacement formulation was used by Monforton and Schmit.[12] The linear-strain triangular element was applied to study the extent of the validity of the Saint-Venant principle in the case of a sandwich strip.[13] Khatua and Cheung developed a triangular element[14] and rectangular element[15] to study the multilayer sandwich plates for their bending and vibration behavior. A finite-element procedure was established for the analysis of sandwich plates with different anisotropic composite facings due to aerodynamic and thermal loads by Weinstein et al.[16] Six-node triangular and eight-node quadrilateral elements are used for the analysis and optimum design of sandwich constructions by Ding,[17] taking the thicknesses of the faces and core as design variables. A simple isoparametric finite element formulation based on a displacement model to account for the nonlinear variation of in-plane displacements and constant transverse displacement through sandwich thickness was presented by Pandya and Kant[18] for the flexural analysis of multilayer symmetric sandwich plates. An initial stress stiffness matrix applicable to the plate elements of arbitrary quadrilateral shape with 12 degrees of freedom was formulated by Cook[19] and applied to the study of the buckling behavior of sandwich plates.

Hybrid-stress finite elements have been developed for the improved analysis based on a modified complementary energy principle in which the intraelement equilibrating stresses and displacements compatible over the entire volume of an element or at the element boundary only are interpolated independently. Cook[20] developed two general quadrilateral hybrid-stress elements having 12 degrees of freedom, one with nine stress parameters and the other with five stress parameters. The shear strain is assumed constant over the thickness of the plate. A stiffness matrix was derived by Kraus[21] for a 5-degree-of-freedom rectangular orthotropic plate element with thick faces by the assumed hybrid-stress approach. In the work of Cook and Kraus, displacements are assumed at the boundary of the element, compatible with the neighboring elements, and the variational functional derived by Pian[22] is used. An eight-node hybrid element with 55 stress parameters for each layer was developed by Liou and Sun[27] to study laminated plates; however, its behavior with respect to invariance, shear-locking, and spurious energy modes is not reported. Spilker[23,24] developed an eight-node hybrid-stress element for the analysis of laminated plates; the equilibrating state of stress is characterized by 67 stress parameters, and a

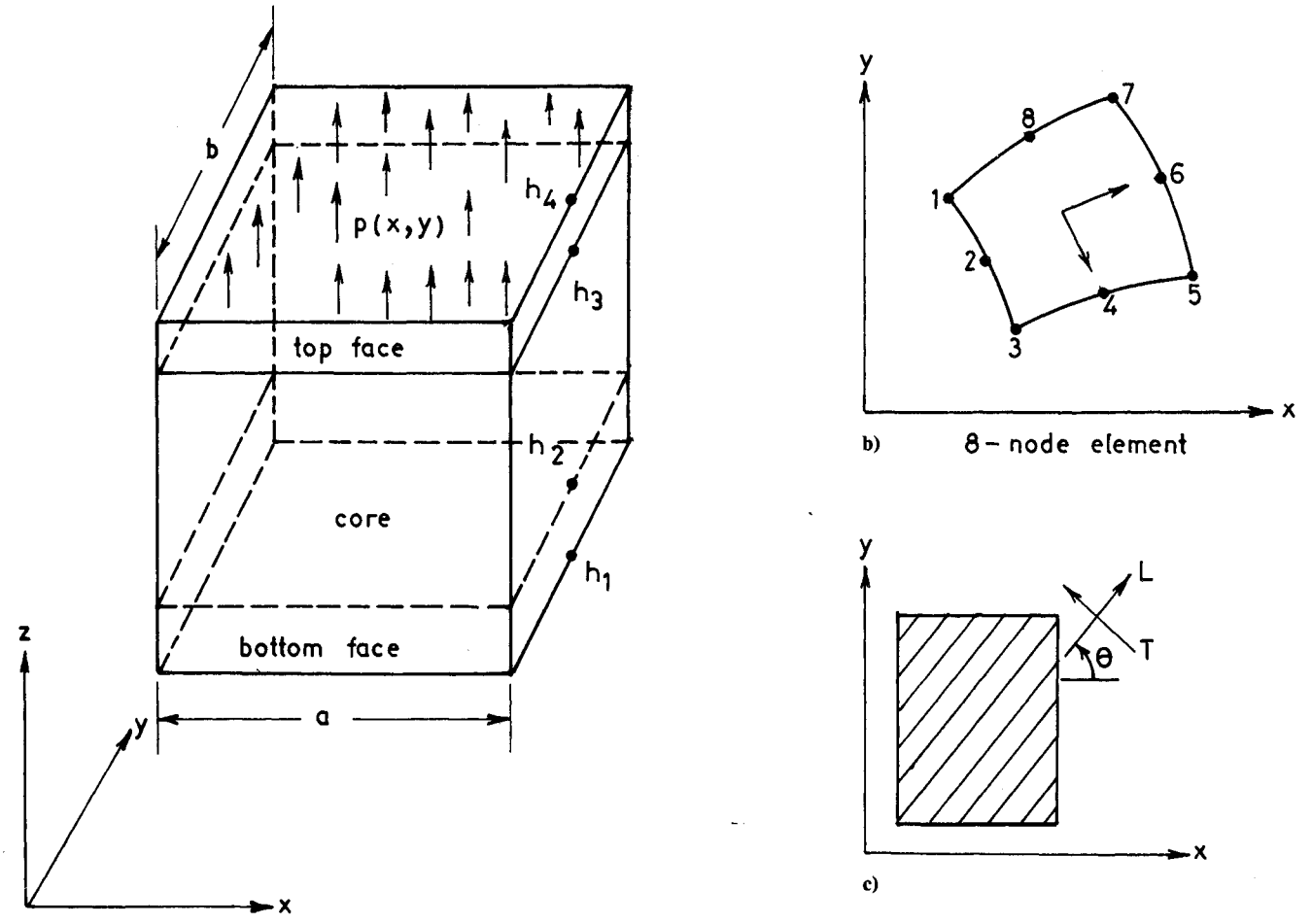

Fig. 1 Geometry.

different shear strain is taken in each layer. Hence, the number of element stress parameters and nodal degrees of freedom is dependent on the number of layers.

In the present analysis, the eight-node quadrilateral quadratic isoparametric element based on the hybrid-stress formulation of Spilker[24] is selected because of its improved performance. In the case of a sandwich plate made of linear elastic materials, the present analysis does not impose any restriction on the geometric and material properties of the faces and core. The displacement and transverse stress continuity at the interfaces and traction-free conditions on the boundary surfaces are exactly satisfied. The element[24] is naturally invariant with respect to coordinate transformation, nonlocking in the thin plate limit, and the element is of the correct rank, which was not verified in the case of hybrid-stress elements used earlier for the analysis of sandwich plates.

II. Formulation

The geometry and coordinate system are given in Fig. 1. The plane of the sandwich plate coincides with the xy plane. The locations of layer surfaces are given by $z = h_1, h_2, h_3$, and h_4, starting from the bottom. The element and node numbering is shown in Fig. 1b; the element shape functions are not listed here, as they are well established elsewhere.[25] The plate is acted on by distributed force vector $p_i(x, y)$ on its boundary surfaces. The functional Π for the hybrid-stress formulation is given by[24]

$$\Pi = \sum_{n=1}^{N} \sum_{i=1}^{3} \left\{ \frac{1}{2} \int_{V_{ni}} \sigma_i^T S_i \sigma_i \, dV - \int_{V_{ni}} \sigma_i^T \epsilon_i \, dV + \int_{A_{ni}} U^{iT} \bar{p}_i \, dA \right\} \tag{1}$$

where

σ_i = assumed stress vector of ith layer,

$$\left[\sigma_x^i, \sigma_y^i, \sigma_z^i, \tau_{yz}^i, \tau_{xz}^i, \tau_{xy}^i\right]^T$$

S_i = transformed compliance matrix of ith layer[26] referred to in geometric axes (x, y, z)

ϵ_i = engineering strain vector of ith layer calculated from assumed displacements u, v, w,

$$\left[\epsilon_x^i, \epsilon_y^i, \epsilon_z^i, \epsilon_{yz}^i, \epsilon_{xz}^i, \epsilon_{xy}^i\right]^T$$

U^i = displacement vector $[u^i, v^i, w]^T$

V_{ni} = volume of ith layer in element n

p_i = external force vector on ith layer

A_{ni} = area of nth element in xy plane occupied by ith layer

N = number of elements

The equilibrating stress vector σ_i, given explicitly in Ref. 24, assumed in the ith layer is written in matrix form as

$$\sigma_i = P_i(x, y, z)\beta^i \tag{2}$$

where

β^i = stress parameter vector of layer i $[\beta_1, \beta_2, \beta_3, \ldots, \beta_{67}]^{iT}$

P_i = 6 × 67 matrix formed of polynomial terms in x, y, z with the σ_i of Ref. 24

The elements of P_i are usually converted into normalized coordinates (ξ, η, ζ) with the help of isoparametric coordinate transformation relations

$$x = \sum_{j=1}^{8} N_j(\xi, \eta)x$$

$$y = \sum_{j=1}^{8} N_j(\xi, \eta)y_j \tag{3}$$

where $N_j(\xi, \eta)$ are the biquadratic serendipity-shaped functions,[25] (x_j, y_j) are the global coordinates of the jth node, and ζ is the transverse normalized coordinate related to z by

$$z = \tfrac{1}{2}[(h_i + h_{i+1}) + \zeta(h_{i+1} - h_i)] \tag{4}$$

so that $\zeta = -1$ at the bottom and $\zeta = +1$ at the top of layer i.

The in-plane displacements u^i and v^i are assumed to vary linearly over each layer and the transverse deflection w is taken to be constant over the plate thickness (i.e., $\epsilon_z = 0$). The displacement model of this pattern is capable of taking care of the zig-zag deformed configuration of adjacent layers in thick laminates (i.e., for width-to-thickness ratio a/h up to, say, 4). The displacements u^i, v^i, and w can be interpolated in terms of their nodal values $(u^i, v^i, w)_j$ in the ith layer as

$$u^i(\xi,\eta,\zeta) = \sum_{j=1}^{8} N_j(\xi,\eta)\left[\frac{1}{2}(1-\zeta)u_j^i + \frac{1}{2}(1+\zeta)u_j^{i+1}\right] \tag{5a}$$

$$v^i(\xi,\eta,\zeta) = \sum_{j=1}^{8} N_j(\xi,\eta)\left[\frac{1}{2}(1-\zeta)v_j^i + \frac{1}{2}(1+\zeta)v_j^{i+1}\right] \tag{5b}$$

$$w(\xi,\eta) = \sum_{j=1}^{8} N_j(\xi,\eta)w_j \tag{5c}$$

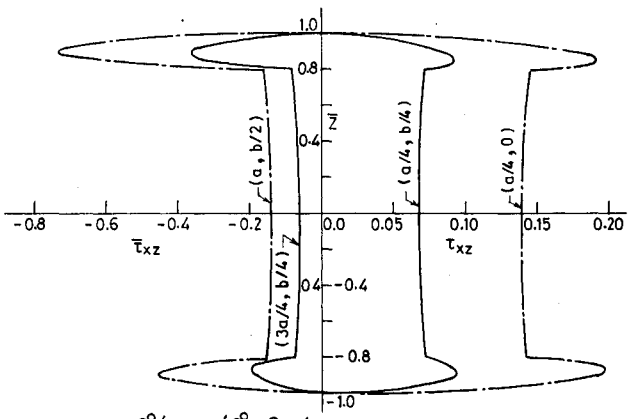

a)

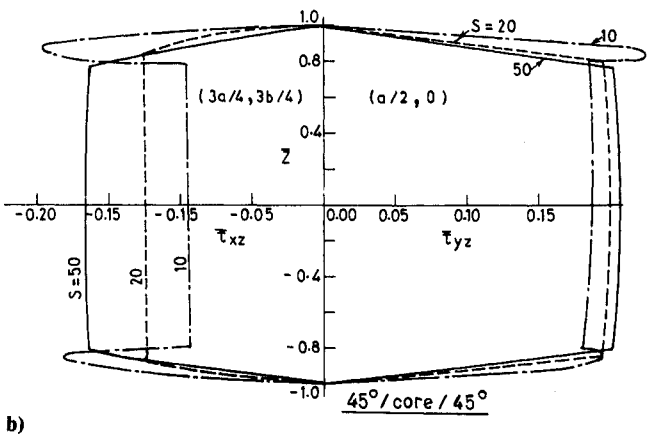

b)

Fig. 2 Variation of $\bar{\tau}_{yz}$ and $\bar{\tau}_{zx}$ over thickness (0.1/0.8/0.1, *SS*, *SL*).

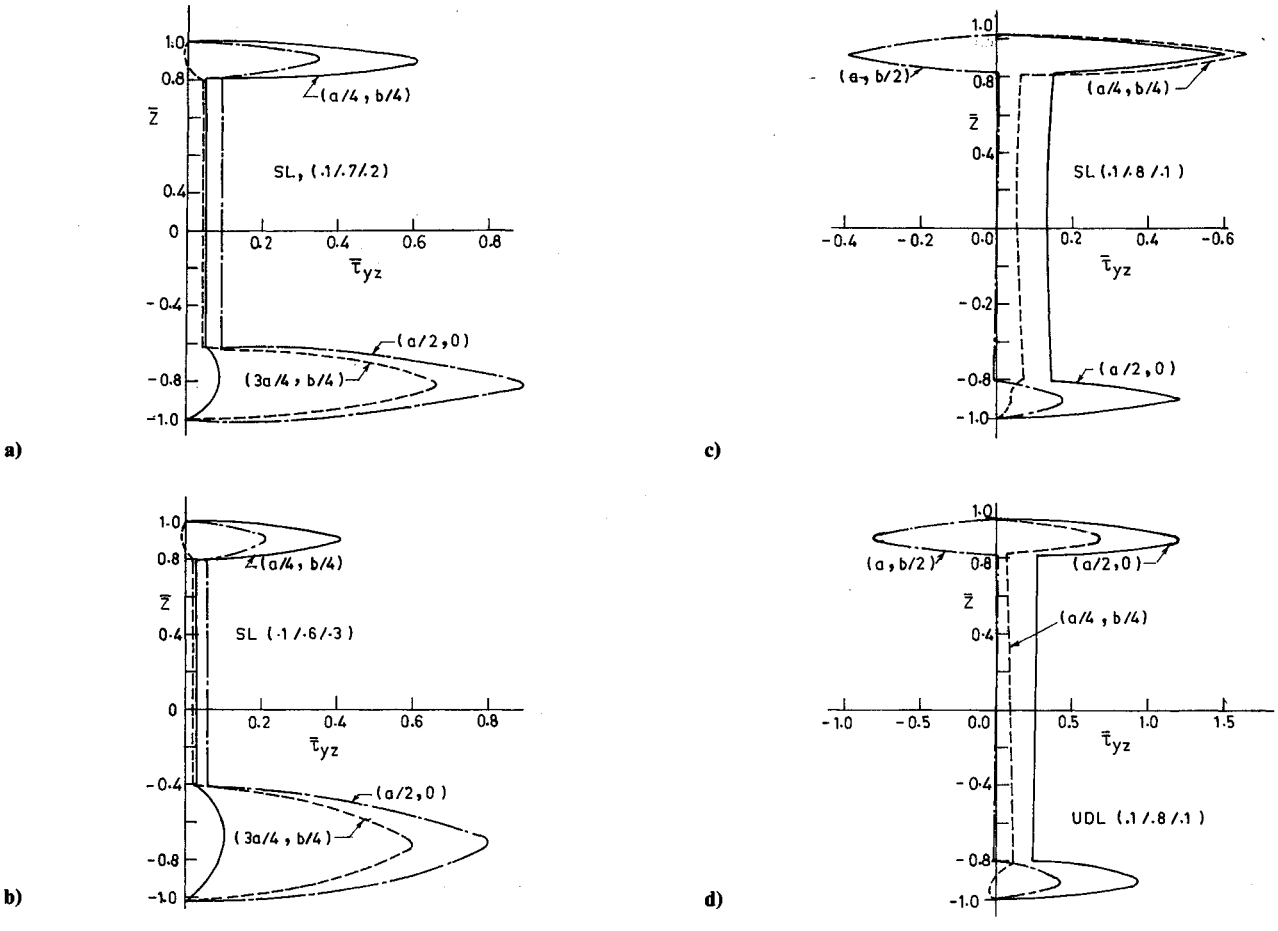

Fig. 3 Variation of $\bar{\tau}_{yz}$ over thickness ($S = 4$, -45 /core/ $+45$ deg, *SS*).

where $(u^i, u^{i+1}, v^i, v^{i+1}, w)_j$ are the values of u^i, v^i, and w at the bottom and top surfaces of layer i at the node j and may be treated as vector q^i of the nodal degrees of freedom of the ith layer

$$q^i = \left[u_1^i, u_1^{i+1}, v_1^i, v_1^{i+1}, w_1, u_2^i, u_2^{i+1}, \ldots, w_2, \ldots, u_8^i, u_8^{i+1}, v_8^i, v_8^{i+1}, w_8\right] \tag{6}$$

Thus, at each node in the case of a three-layered sandwich, there are nine degrees of freedom; the element nodal displacement vector q consists of 72 components in the present situation and is arranged as shown here.

$$q = \left[u_1^1, u_1^2, u_1^3, u_1^4, v_1^1, v_1^2, v_1^3, v_1^4, w_1, u_2^1, \ldots, w_2, \ldots, u_8^1, u_8^2, u_8^3, u_8^4, v_8^1, v_8^2, v_8^3, v_8^4, w_8\right]^T \tag{7}$$

With the help of Eqs. (5) and the definition of the ith layer nodal displacement vector q^i in Eq. (6), the layer displacement vector U^i defined by

$$U^i = [u^i, v^i, w]^T \tag{8}$$

can be cast into matrix form

$$U^i = N^i q^i \tag{9}$$

where N^i is a 3×40 matrix, and its elements are dependent on the shape functions N_j and normalized coordinate ζ. By using the displacement vector of Eq. (9) in the linear-strain displacement relations, the strain vector ϵ_i can be related to q^i by

$$\epsilon_i = B^i q^i \tag{10}$$

where B^i is the strain matrix of the ith layer that can be obtained with the help of Eqs. (5), (6), and (9).

By substituting Eqs. (2), (9), and (10) in Eq. (1) and using the following definitions of layer matrices:

$$H^i = t_i \int_{-1}^{1}\int_{-1}^{1}\int_{-1}^{1} P_i^T S_i P_i |J| \, d\xi \, d\eta \, d\zeta \tag{11a}$$

$$G^i = t_i \int_{-1}^{1}\int_{-1}^{1}\int_{-1}^{1} P_i^T B^i |J| \, d\xi \, d\eta \, d\zeta \tag{11b}$$

$$Q^i = \int_{A_{ni}} N^{iT} \bar{p}^i |J| \, d\xi \, d\eta \tag{11c}$$

the variational functional Π becomes

$$\Pi = \sum_{n=1}^{N} \sum_{i=1}^{3} \left\{\frac{1}{2}\beta^{iT} H^i \beta^i - \beta^{iT} G^i q^i + q^{iT} Q^i\right\} \tag{12}$$

In Eq. (11), J is the Jacobian of the coordinate transformation of Eq. (3), and t_i is half the thickness of the ith layer given by

$$t_i = \frac{h_{i+1} - h_i}{2} \tag{13}$$

The stress parameters β_j in the expression of stresses listed in Ref. 24 are already adjusted to satisfy the static equilibrium equations. They are now to be further adjusted to satisfy the traction-free boundary conditions and the transverse stress continuity conditions at the interfaces. As a result, the following interrelations between β_j^i and β_j^{i-1} $(i > 1)$ will be found at the interfaces $z = h_2$ and $z = h_3$.

$$\beta_j^i = \frac{t_{i-1}}{t_i} \beta_{j+52}^{i-1} \qquad \text{for} \qquad i = 2,3 \text{ and } j = 1,2,\ldots,12 \tag{14a}$$

Table 1 Maximum stresses and deflections in three-layered rectangular ($b = 3a$) laminate[a]

a/h		$\bar{\sigma}_x(a/2, b/2, \pm 1)$	$\bar{\sigma}_y(a/2, b/2, \pm 1/3)$	$\bar{\tau}_{zx}(a, b/2, 0)$	$\bar{\tau}_{yz}(a/2, b, 0)$	$\bar{\tau}_{xy}(a, b, \pm 1)$	$\bar{w}(a/2, b/2, 0)$
4	HFE[a]	0.934	0.107	0.387	0.0380	−0.0266	2.752
		−0.990	−0.109	0.422(5/12)[c]	—	0.0276	
	EL[b]	1.10	0.109	0.351	0.0334	−0.0269	2.820
		−1.14	−0.119	0.387(0.54)	—	0.0281	
10	HFE	0.695	0.037	0.454	0.0205	−0.0123	0.916
		−0.711	−0.0366	—	—	0.0124	
	EL	0.726	0.0418	0.420	0.0152	−0.0120	0.919
		−0.725	−0.0435	—	—	0.0123	
20	HFE	0.644	0.0256	0.472	0.0165	−0.00927	0.608
		−0.647	−0.0257	—	—	0.00934	
	EL	±0.650	0.0294	0.432	0.0119	∓0.0093	0.610
			−0.0299	—	—		
50	HFE	±0.627	±0.0233	0.490	0.0137	∓0.00824	0.519
	EL	±0.628	±0.0259	0.439	0.0110	∓0.00840	0.520
100	HFE	±0.623	±0.0229	0.496	0.0120	∓0.00801	0.506
	EL	±0.624	±0.0253	0.439	0.0108	∓0.00830	0.508

[a]Finite element saturation. [b]Elasticity solution. [c]Value of $\bar{z}$ where $\bar{\tau}_{zx}$ is max.

$$\beta_j^i = \frac{t_{i-1}^2}{t_i^2}\,\beta_{j+52}^{i-1} \qquad \text{for} \qquad i = 2,3 \text{ and } j = 13,14,15 \tag{14b}$$

If we assume that the sandwich plate is subjected to only a transverse distributed force of intensity $p(x, y)$ at the surface ($z = h_4$), the traction-free boundary conditions then are

$$\sigma_z^1 = \tau_{yz}^1 = \tau_{zx}^1 = 0 \qquad \text{at} \qquad z = h_1$$

$$\tau_{yz}^3 = \tau_{zx}^3 = 0 \qquad \text{at} \qquad z = h_4 \tag{15a}$$

that require that

$$\beta_j^1 = 0 \qquad \text{for} \qquad j = 1,2,\ldots,15$$

$$\beta_j^3 = 0 \qquad \text{for} \qquad j = 53,54,\ldots,64 \tag{15b}$$

The collection of stress parameters of all three layers in a typical element after being subjected to the condition of Eqs. (14) and (15) yields an independent laminate stress parameter vector β as

$$\beta = \left[\beta_{16}^1,\beta_{17}^1,\ldots,\beta_{67}^1,\beta_{16}^2,\beta_{17}^2,\ldots,\beta_{67}^2,\beta_{16}^3,\beta_{17}^3,\ldots,\right.$$
$$\left.\beta_{52}^3,\beta_{65}^3,\beta_{66}^3,\beta_{67}^3\right]^T \tag{16}$$

The layer nodal displacement vector q^i can be related to element nodal displacement vector q, and the layer stress parameter vector β^i to element stress parameter vector β by

$$q^i = C_d^i q \tag{17a}$$

$$\beta^i = C_S^i \beta \tag{17b}$$

where C_d^i and C_S^i are the Boolean matrices with zero or unit as the values of its elements.

By substituting Eq. (17) in Eq. (12) and using the definitions

$$H = \sum_{i=1}^{3} C_S^{iT} H^i C_S^i \tag{18a}$$

$$G = \sum_{i=1}^{3} C_S^{iT} G^i C_d^i \tag{18b}$$

$$Q = \sum_{i=1}^{3} C_d^i Q^i \tag{18c}$$

the expression for Π becomes

$$\Pi = \sum_{n=1}^{N} \left\{\frac{1}{2}\beta^T H \beta - \beta^T G q + q^T Q\right\} \tag{19}$$

In Eq. (19) q and β are the independent field parameters with respect to which the functional Π must be extremized. Extremizing it with respect to β and solving the resulting equations, one gets

$$\beta = H^{-1} G q \tag{20}$$

thus paving the way to express the element stress parameters β in terms of nodal displacements q. The elimination of β in Eq. (19) by means of Eq. (20) results in

$$\Pi = -\sum_{i=1}^{N} \left\{\frac{1}{2} q^T G^T H^{-1} G q - q^T Q\right\} \tag{21}$$

The element stiffness matrix k is then given by

$$k = G^T H^{-1} G \tag{22}$$

In the present case, the element load vector Q takes the form

$$Q = \int_{-1}^{1}\int_{-1}^{1} [0,0,0,0,0,0,0,0,0,N_1 p,0,0,\ldots,N_2 p,\ldots,$$
$$0,0,0,0,0,0,0,0,N_8 p]^T J \, d\xi \, d\eta \tag{23}$$

The layer matrices H^i, G^i, and Q^i of Eq. (11) are numerically evaluated using a $4 \times 4 \times 4$ Gauss quadrature rule and then assembled to obtain element matrices H, G, and Q. The LDL^T decomposition of the solution technique is used to get the inverse of H and the product $H^{-1}G$ in Eq. (22). Finally, a frontal solution technique is adopted to solve for the global displacements.

III. Numerical Results

The formulation and computer program developed by the authors were checked by comparing the results of the present

solution with the three-dimensional elasticity solution of Ref. 5. The results, listed in Table 1 for comparison, are for a three-layered rectangular laminate subjected to sinusoidal load and simply supported. The material properties used are those given in Ref. 5. The layers of the rectangular laminate are of equal thickness and of a fiber orientation (0/90/0 deg) and have the following material properties:

$$E_L = 25 \times 10^6 \text{ psi } (\cong 0.175 \times 10^6 \text{ N mm}^2)$$

$$E_T = 10^6 \text{ psi } (\cong 0.7 \times 10^4 \text{ N mm}^2)$$

$$G_{LT} = 0.5 \times 10^6 \text{ psi } (\cong 0.35 \times 10^4 \text{ N mm}^2)$$

$$G_{TT} = 0.2 \times 10^6 \text{ psi } (\cong 0.14 \times 10^4 \text{ N mm}^2)$$

$$\mu_{LT} = \mu_{TT} = 0.25 \tag{24}$$

The results presented with overbars are the normalized quantities according to the scheme

$$(\bar{\sigma}_x, \bar{\sigma}_y, \bar{\tau}_{xy}) = \frac{1}{p_0 S^2} (\sigma_x, \sigma_y, \tau_{xy})$$

$$(\bar{\sigma}_z, \bar{\tau}_{yz}, \bar{\tau}_{zx}) = \frac{1}{p_0 S} (\sigma_z, \tau_{yz}, \tau_{zx})$$

$$(\bar{u}, \bar{v}) = \frac{E_T}{phS^3} (u, v), \qquad \bar{w} = \frac{100 E_T}{phS^4} w$$

$$S = \frac{a}{h}, \qquad \bar{z} = \frac{2z}{h} \tag{25}$$

The response of a simply supported and clamped square sandwich plate is studied by varying the parameters like the fiber orientation angle θ measured from the x axis, the width-to-thickness ratio ($S = a/h$), laminate unsymmetricity, and two different distributions of loading. The simply supported conditions are defined by taking at the edges the deflection w and the in-plane displacements parallel to the edges' zero, and for the clamped condition all the layer surface displacements are zero at the boundaries. The face materials are characterized by the properties listed in Eq. (24), and the core is made of Rohacell-71 foam characterized by the following properties:

$$E_{xx} = E_{yy} = E_{zz} = 0.145 \times 10^5 \text{ psi } (\cong 100 \text{ N mm}^2)$$

$$G_{xz} = G_{yz} = G_{xy} = 0.58 \times 10^4 \text{ psi } (\cong 40 \text{ N mm}^2)$$

$$\mu_{xy} = \mu_{yz} = \mu_{zx} = 0.25 \tag{26}$$

In the figures, B stands for the bottom layer, T for the top layer, C for the core, SS for simply supported, CC for clamped, SL for sinusoidal load, and UDL for uniformly distributed load. The fiber orientation in the top and bottom faces is denoted by $\mp\theta$ or $\pm\theta$, where the top sign corresponds to the top face and the bottom sign to the bottom face. The layer thickness fractions in the sandwich are denoted by ($n_3/n_2/n_1$), e.g., (0.1/0.7/0.2) means the volume fractions of the top, core, and bottom layers, respectively, are 0.1, 0.7 and 0.2. Whenever symmetry exists, a quarter plate is discretized; with arbitrary fiber orientation, the full plate is discretized. The 2×2 and 4×4 meshes are used for quarter and full

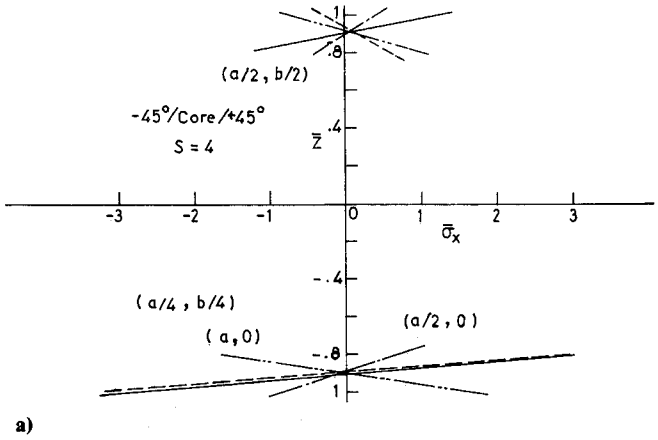

a)

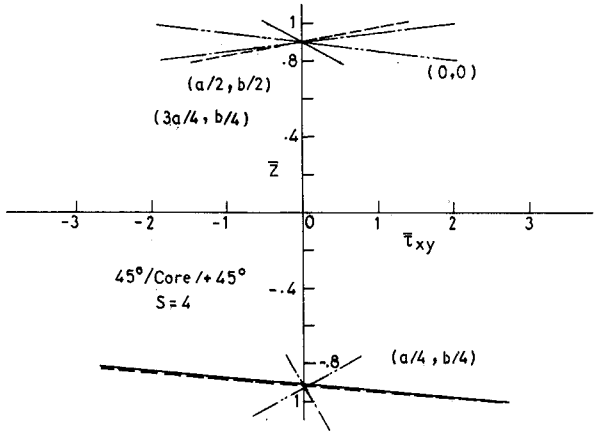

b)

Fig. 4 Variation of in-plane stresses over thickness (0.1/0.8/0.1, *SS*, *SL*).

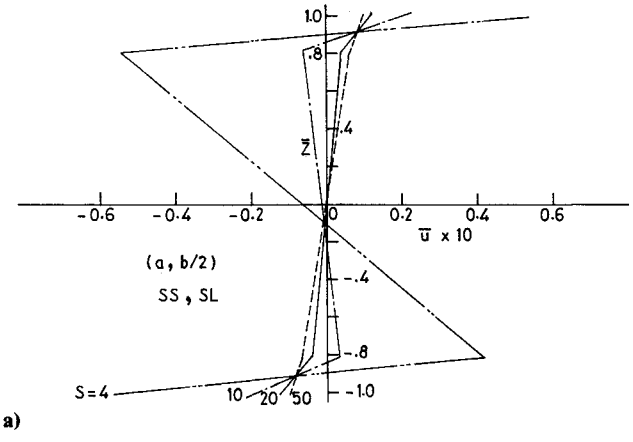

a)

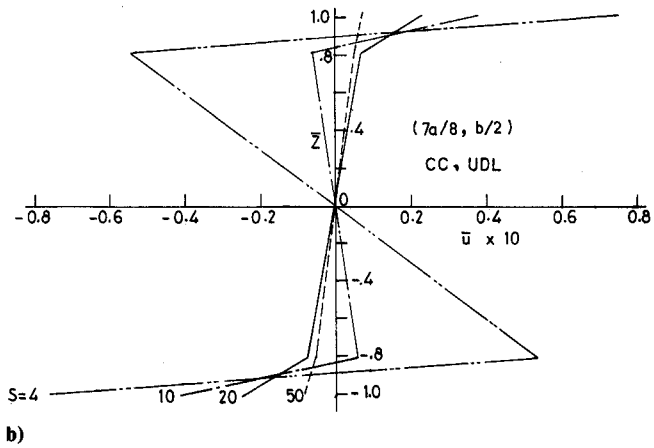

b)

Fig. 5 Variation of $\bar{u}$ over thickness (+45 /core/+45 deg, 0.1/0.8/0.1).

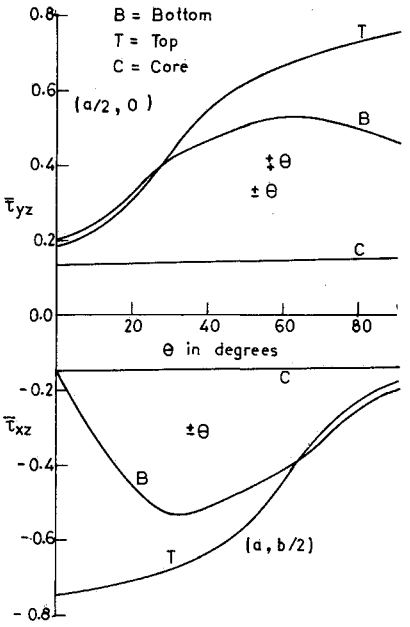

Fig. 6 Variation of transverse shear stresses in the middle of layers with θ ($S = 4$, 0.1/0.8/0.1, *SS*, *SL*).

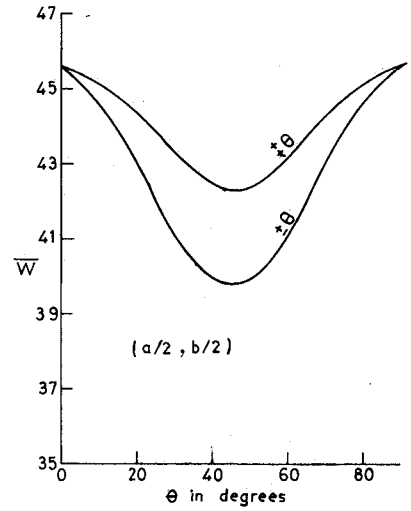

Fig. 7 Variation of central deflection $\bar{w}$ with θ ($S = 4$, 0.1/0.8/0.1, *SS*, *SL*).

plates, respectively. The rectangular plate ($b = 3a$) with symmetry is discretized with a 2×6 mesh in one quarter. The values used to plot the graphs are their averages obtained from all of the elements meeting at the point of interest.

IV. Discussion

The results of the present solution are very close to those of the three-dimensional elasticity solution, as shown in Table 1.

Figures 2 and 3 illustrate the variation of the transverse shear stresses $\bar{\tau}_{zx}$ and $\bar{\tau}_{yz}$ over the thickness at different cross sections of a simply supported square sandwich plate. In the case of thicker plates ($S = 4$, Figs. 2a, 3c, and 3d), the transverse shear stress is higher in the faces than in the core. This is more so in a plane in which the faces are stiffer because of fiber orientation, as is seen in Fig. 2a from the comparison of the graphs of $\bar{\tau}_{zx}$ and $\bar{\tau}_{yz}$. As a result, the faces are subjected to bending action about their own centroidal axis that can be observed from the nature of distribution of in-plane stresses in Fig. 4. With the decrease of plate thickness, the shear stresses gradually increase from the outer surface to the inner surface of the faces and finally become maximum at the center of the core (Fig. 2b, $S = 20$ and 50). For values of S greater than about 20, the transverse shear stresses are maximum in the core, and the major part of the shear is resisted by the core, and the faces tend to the membrane state, provided they are sufficiently thin compared to the core. At some cross sections [point ($a/4$, $b/4$) of Figs. 3c and 3d], the top face on the convex side is heavily sheared and the bottom face on the concave side is undersheared. The transverse shear $\bar{\tau}_{yz}$ at the point (a, $b/2$) in Fig. 3c is negative in the top face on the convex side and positive in the bottom face on the concave side; at such cross sections, the nature of bending action in the faces opposses each other (Fig. 4a). For the sandwich with faces of unequal thickness, the shear stress $\bar{\tau}_{yz}$ is higher at certain cross sections, say, point ($a/4$, $b/4$) of Figs. 3a and 3b, in the thinner face; at certain other cross sections, say, points ($a/2$, 0) and ($3a/4$, $b/4$) of Figs. 3a and 3b, the thicker faces carry maximum shear force. In general, the shear stress in the core decreases as the faces become thicker (Fig. 3).

In the case of thick sandwiches (Figs. 4a and 4b), the faces act almost as two independent plates. At some cross section [($a/2$, $b/2$) and ($a/2$, 0) of Fig. 4a], they help each other to resist the bending action and oppose each other at certain other cross sections [($a/4$, $b/4$) of Fig. 4a], whereas for thin sandwiches, the bending action of both faces adds up to resist the bending loads. The values of a particular in-plane stress ($\bar{\sigma}_x$, $\bar{\sigma}_y$, or $\bar{\tau}_{xy}$) in both faces differ considerably in the case of a thick sandwich, but are closer in the case of a thin sandwich. The in-plane shear stress $\bar{\tau}_{xy}$ is found to be maximum in the bottom face of a generally orthotropic sandwich at the point ($a/4$, $b/4$) of Fig. 4b, which would occur at the corner points in the case of isotropic and cross-ply face sandwiches and thin sandwiches with the simply supported boundary conditions.

The deformed cross sections of a simply supported sandwich under a sinusoidal load and of a clamped sandwich under a uniformly distributed transverse load are shown in Figs. 5a and 5b, respectively. The warping of the cross section is severe for a value of $S < 50$. As is observed in Fig. 5, the warping is almost zero at $S = 50$ and the cross sections remain plane after deformation, in which case lower-order bending theories can yield a sufficiently accurate solution.

The variation of the sandwich plate response with the change of fiber orientation θ in the faces is presented in Figs. 6–9. The transverse shear stresses plotted in Fig. 6 are their values in the mid-planes of the layers. The influence of fiber orientation angle θ in the face sheets on the value of transverse shear stress in the core (Fig. 6) is almost negligible. At the cross sections shown in Fig. 6, the shear stress $\bar{\tau}_{yz}$ is higher in the bottom face for θ less than 27 deg, and τ_{xz} is higher in the

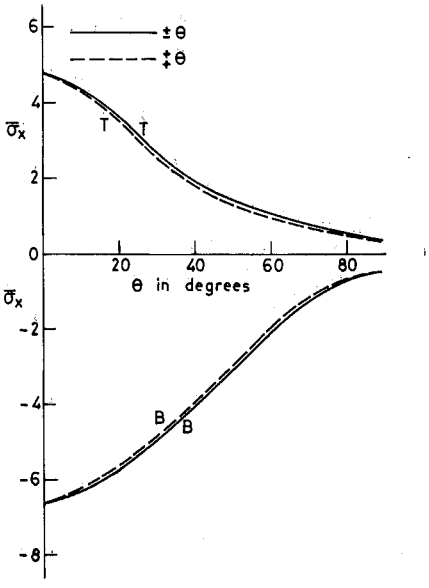

Fig. 8 Variation of $\bar{\sigma}_x$ with θ ($S = 4$, 0.1/0.8/0.1, *SS*, *SL*).

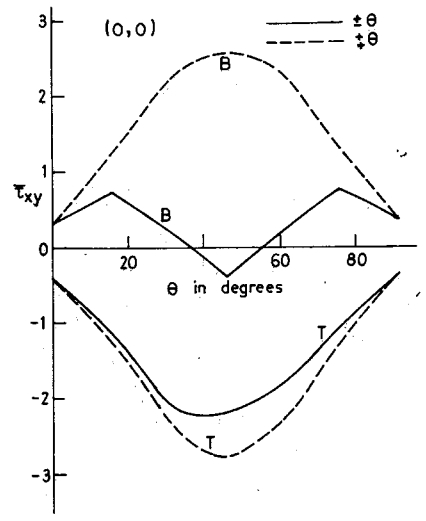

a)

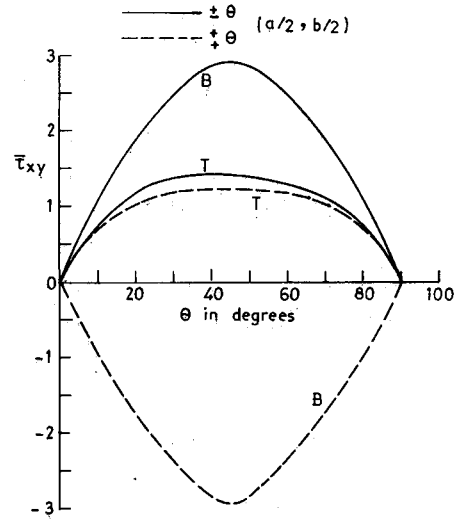

b)

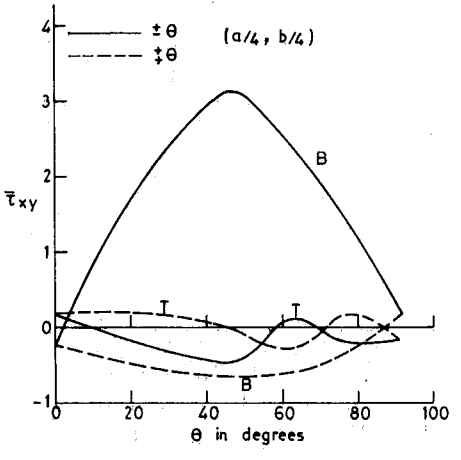

c)

Fig. 9 Variation of $\bar{\tau}_{xy}$ in the top and bottom surfaces with θ ($S = 4$, 0.1/0.8/0.1, *SS*, *SL*).

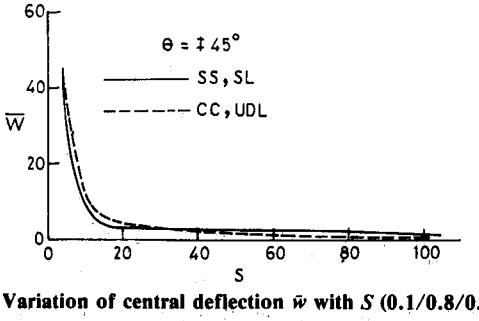

Fig. 10 Variation of central deflection $\bar{w}$ with S (0.1/0.8/0.1).

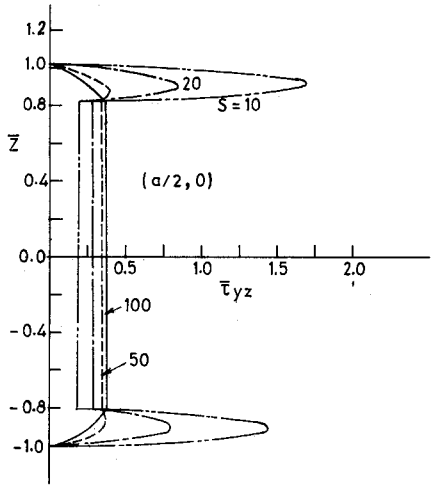

Fig. 11 Variation of $\bar{\tau}_{yz}$ over thickness (+45 /core/ +45 deg, 0.1/0.8/0.1, *CC*, *UDL*).

top face for θ less than 63 deg. When the fibers are oriented along the x axis, the shear stress $\bar{\tau}_{zx}$ at the point $(a, b/2)$ is almost zero in the bottom and very high in the top face (Fig. 6). The difference decreases with an increase in the value of θ. The difference in values of $\bar{\tau}_{yz}$ in the top and bottom faces is large when the fibers are placed closer to the y axis.

The central deflection and central in-plane stress in the boundary surfaces, respectively, of a square sandwich plate for two different fiber orientations $\pm\theta$ and $\pm\theta$ are plotted in Figs. 7 and 8. The symmetric angle-ply ($\pm\theta$ curve) deflects more than the antisymmetric angle-ply ($\pm\theta$ curve) sandwich. However, the difference in the maximum values of the central bending stresses for these two patterns of fiber orientations is very small (Fig. 8). For a fiber orientation $0 \le \theta \le 90$ deg, the value of $\bar{\sigma}_x$ is higher in the top face.

The variation of in-plane shear stress $\bar{\tau}_{xy}$ at the outer surfaces with a fiber orientation angle θ for the two orientation patterns at the points (0, 0), $(a/2, b/2)$, and $(a/4, b/4)$ is plotted in Fig. 9. The influence of fiber orientation patterns ($\pm\theta$ and $\pm\theta$) over the values of $\bar{\tau}_{xy}$ in the top surface (T curves) is negligibly small compared to that in the bottom surface (B curves). The $\bar{\tau}_{xy}$ is higher in the bottom surface than in the top surface for $0 < \theta < 90$ deg as in the case of in-plane normal stress $\bar{\sigma}_x$.

Figure 10 shows the variation of the normalized central deflection $\bar{w}$ of a simply supported plate under sinusoidal loading and of a clamped plate under uniformly distributed loading with the width-to-thickness ratio S.

The behavior of a clamped square sandwich plate subjected to a uniformly distributed load is presented in Fig. 11. The shear stresses (say, $\bar{\tau}_{yz}$ of Fig. 11) in the core are much less than in the faces of the clamped thick sandwich, compared to that observed in the case of a simply supported sandwich (Figs. 3c and 3d). The maximum shear stress occurs at the centers of the faces. As the plate becomes thinner, the shear stresses gradually increase in the faces from the outer surface to the inner one; then they become maximum at the center of the core (Fig. 11, $S = 100$ curve). For a simply supported sandwich, the maximum shear stress occurs when the value of S is greater than 20 (Fig. 2b), but for the clamped sandwich even when the value of S is 50, $\bar{\tau}_{yz}$ in the faces is higher than in the core (Fig. 11).

V. Conclusions

The behavior of a thick angle-ply FRP-faced sandwich is very sensitive to various inherent parameters like the relative thicknesses of faces and core, fiber orientation angle θ, boundary restraint conditions, etc. It is difficult to arrive at a definite conclusion regarding a particular observation, say, the location where a certain stress reaches its maximum value.

Within the limitations of the parametric study made in this paper, the following conclusions can be drawn.

1) In the case of an angle-ply FRP-faced thick sandwich, the core does not carry the shear force as much as is expected in a sandwich. This is true more so for the clamped conditions. The faces carry the bulk of the shear force and are subjected to bending action about their own centroidal axis. They no longer act as membranes as expected in a sandwich. The nature of shear force, bending moment, and twisting moment in the two faces differs widely. The values of any of the specific stress-resultants for these three in the two faces may add up to or oppose each other. The value of the in-plane shear $\bar{\tau}_{xy}$ in a clamped square sandwich is maximum at point $(a/2, 0)$, in contrast to isotropic and cross-ply faced sandwiches and thin sandwiches, irrespective of the face material where $\bar{\tau}_{xy}$ is maximum at the center point $(a/4, b/4)$ of their quadrants.

2) For the width-to-thickness ratio $S > 20$ in the case of a simply supported sandwich and $S > 50$ in the case of a clamped sandwich, the core comprises almost the entire shear, and the faces act as membranes. Therefore, to achieve the expected economy of the sandwich construction, it is recommended that the thickness parameter S be adjusted whenever possible.

3) The central deflection is minimum when the fiber orientation angle (θ) is $+45$ deg in the top face and -45 deg in the bottom face.

4) The warping of the sandwich cross section is almost negligible for $S > 50$.

References

[1]Reissner, E., "Small Bending and Stretching of Sandwich-Type Shells," NACA Rept. TN 1526 and also NACA Rept. 899, 1948.

[2]Yu, Y.-Y., "A New Theory of Elastic Sandwich Plates—One-Dimensional Case," *ASME Journal of Applied Mechanics,* Vol. 26, 1959, pp. 415–421.

[3]Hoff, N. J., "Bending and Buckling of Rectangular Sandwich Type Shells," NACA Rept. 925, 1950.

[4]Srinivas, S., and Rao, A. K., "Bending Vibration and Buckling of Simply Supported Thick Orthotropic Rectangular Plates and Laminates," *International Journal of Solids and Structures,* Vol. 6, 1970, pp. 1463–1481.

[5]Pagano, N. J., "Exact Analysis for Rectangular Bidirectional Composites and Sandwich Plates," *Journal of Composite Materials,* Vol. 4, 1970, pp. 20–34.

[6]Whitney, J. M., "Stress Analysis of Thick Laminated Composite and Sandwich Plates," *Journal of Composite Materials,* Vol. 6, 1972, pp. 426–440.

[7]Rao, D. K., "Static Response of Stiff-Cored Unsymmetric Sandwich Beams," *ASME Journal of Engineering for Industry,* Vol. 43, 1976, pp. 391–396.

[8]Rao, K. M., "Buckling Coefficients for FRP Faced Sandwich Panels Under Combined Loading," *AIAA Journal,* Vol. 25, 1987, pp. 733–739.

[9]Rao, K. M., and Meyer-Piening, H.-R., "Critical Shear Loading of FRP Faced Curved Sandwich Plate," *AIAA Journal,* Vol. 24, 1986, pp. 1531–1536.

[10]Mindlin, R. D., "On Reissner's Equations for Sandwich Plates," *Mechanic Today*, edited by S. Nermat Nasser, Pergamon, Oxford, England, UK, 1980, pp. 315–328.

[11]Rao, N. R., and Valsarajan, K. V., "Large Deflection Analysis of Clamped Skew Sandwich Plates by Parametric Differentiation," *Computers and Structures,* Vol. 17, 1983, pp. 599–602.

[12]Monforton, G. R., and Schmit, L. A., "Finite Element Analysis of Sandwich Plates and Cylindrical Shells with Laminated Faces," *Proceedings 2nd Conference in Matric Meth. Struct. Mech.,* Wright-Patterson AFB, OH, 1969, pp. 573–616.

[13]Rao, N. R., and Valsarajan, K. V., "Saint-Venant's Principle in Sandwich Strip," *Computers and Structure,* Vol. 12, 1980, pp. 185–188.

[14]Khatua, T. P., and Cheung, Y. K., "Triangular Element for Multilayer Sandwich Plates," *Journal of Eng. Mech. Division,* Vol. 98, 1972, pp. 1225–1238.

[15]Khatua, T. P., and Cheung, Y. K., "Bending and Vibration of Multilayer Sandwich Beams and Plates," *International Journal for Numerical Methods in Engineering,* Vol. 6, 1973, pp. 11–24.

[16]Weinstein, F., Putter, S., and Stavsky, Y., "Thermoelastic Stress Analysis of Anisotropic Composite Sandwich Plates by Finite Element Method," *Computers and Structures,* Vol. 17, 1983, pp. 31–36.

[17]Ding, Y., "Optimum Design of Sandwich Constructions," *Computers and Structures,* Vol. 25, 1987, pp. 51–68.

[18]Pandya, B. N., and Kant, T., "Higher-Order Shear Deformable Theories for Flexure of Sandwich Plates—Finite Element Evaluation," *International Journal of Solids and Structures,* Vol. 24, 1988, pp. 1267–1286.

[19]Cook, R. D., "Finite Element Buckling Analysis of Homogeneous and Sandwich Plates," *International Journal for Numerical Methods in Engineering,* Vol. 9, 1975, pp. 39–50.

[20]Cook, R. D., "Two Hybrid Elements for Analysis of Thick, Thin and Sandwich Plates," *International Journal for Numerical Methods in Engineering,* Vol. 5, 1972, pp. 277–288.

[21]Kraus, H. D., "A Hybrid Stiffness Matrix for Orthotropic Sandwich Plates with Thick Faces," *International Journal for Numerical Methods in Engineering,* Vol. 11, 1977, pp. 1291–1306.

[22]Pian, T. H. H., "Derivation of Element Stiffness Matrices by Assumed Stress Distribution," *AIAA Journal,* Vol. 2, 1964, pp. 1333–1336.

[23]Spilker, R. L., "Hybrid-Stress Eight-Node Element for Thin and Thick Multilayer Laminated Plates," *International Journal for Numerical Methods in Engineering,* Vol. 18, 1982, pp. 801–828.

[24]Spilker, R. L., "An Invariant Eight-Node Hybrid-Stress Element for Thin and Thick Multilayer Laminated Plates," *International Journal for Numerical Methods in Engineering,* Vol. 20, 1984, pp. 573–587.

[25]Hinton, E., and Owen, D. R. J., *Finite Element Programming,* Academic Press, London, 1977, pp. 98–107.

[26]Jones, R. M., *Mechanics of Composite Materials,* McGraw-Hill, New York, 1975, pp. 32–60.

[27]Liou, W.-J., and Sun, C. T., "A Three-Dimensional Hybrid Stress Isotropic Element for the Analysis of Laminated Composite Plates," *Computers and Structures,* Vol. 25, 1987, pp. 241–249.